CEFR PHYSICAL START-UP TESTS: THE CORE SPECIFICATIONS AND EXPERIMENTS

X. HUO[1], Y. HU[1], J. ZHANG[1], X. CHEN[1]

[1] China Institute of Atomic Energy, Beijing, China

Email contact of corresponding author: huoxingkai06@163.com

Abstract

China Experimental Fast Reactor (CEFR) is a sodium-cooled fast-spectrum reactor built in China Institute of Atomic Energy, Beijing. The thermal power is 65MW. In the first cycle the reactor core was loaded with uranium dioxide fuel enriched at about 64%. In the physical start-up tests in 2010, a series of experiments were conducted, which not only made an essential part of the reactor start-up, but also produced valuable data for the validation of neutronics codes and nuclear data. In 2018, CIAE proposed an IAEA Coordinated Research Project (CRP) aimed at establishing a benchmark based on the start-up tests. The CRP has drawn 27 participating organizations from all over the world. This paper introduces the main specifications of the CEFR core as well as the procedures and typical measurement results of the selected experiments for the benchmark: the fuel loading and criticality, measurements of control rod worth, sodium void reactivity, temperature reactivity, subassembly swap reactivity, and reaction rate distribution.

1. INTRODUCTION

China Experimental Fast Reactor (CEFR) is a 65MWth pool-type sodium-cooled fast-spectrum reactor located in China Institute of Atomic Energy (CIAE), at southwest suburb of Beijing. In the first cycle it was loaded with uranium dioxide fuel enriched at approximately 64%.

In the physical start-up tests in 2010, four series of low-power experiments were conducted, classified as fuel loading and criticality approaching, measurements of control rod worth, reactivity coefficients, and foil activation. These experiments not only made an essential part of the reactor start-up, but also produced valuable data for the validation of neutronics code and nuclear data. Under the direction and support from International Atomic Energy Agency (IAEA), CIAE proposed the current Coordinated Research Project (CRP) to develop a benchmark based on the start-up tests.

This paper provides the main specifications of the CEFR core and a brief description of the experiments, as well as typical measurement results of each experiment. The full specifications and benchmark analyses can be found in corresponding IAEA CRP documents.[1][2]

2. OVERVIEW OF CEFR

The main parameters of the reactor are listed in TABLE 1. All the parameters are corresponding to the first loading, at installation temperature of 20°C, and in nominal value or design value. The reactor block is shown in FIG. 1. The reactor core configuration and operation involve two main phases: the starting phase, including the first loading and transition loadings; the equilibrium refuelling phase, in which the core layout remains equivalent after each refuelling. The physical start-up tests involved in this benchmark were conducted in the first loading, the layout of which is shown in FIG. 2.

TABLE 1. MAIN PARAMETERS OF CEFR

Parameter	Value
Thermal/electric power, MW	65/20
Designed life, year	30
Maximum burn-up, MWd/t	60,000
Maximum neutron flux, $cm^{-2}s^{-1}$	3.2×10^{15}
Refueling period, day	80
Diameter/height of main vessel, m	8.0/12.2
Covering gas pressure, MPa	0.005
Core inlet/outlet temperature (full power), °C	360/530
SA lattice pitch, mm	61.0
SA outer/inner flat-to-flat dimension, mm	59.0/56.6
Wrapper thickness, mm	1.2

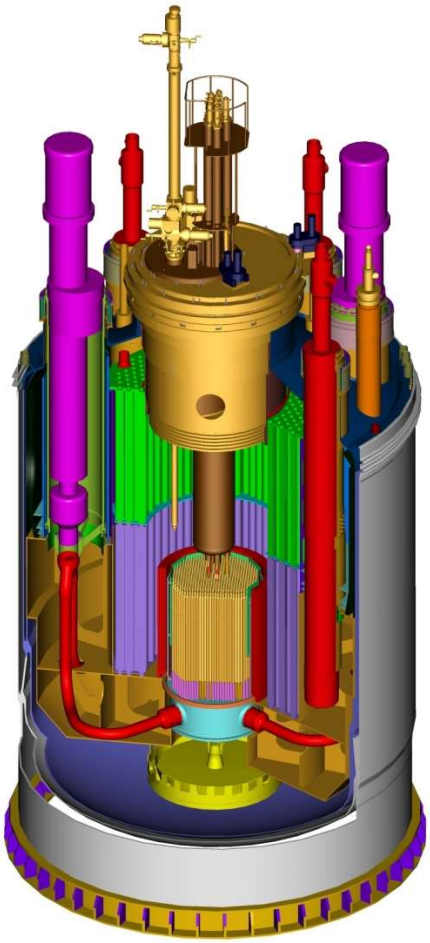

FIG. 1. The reactor block of CEFR

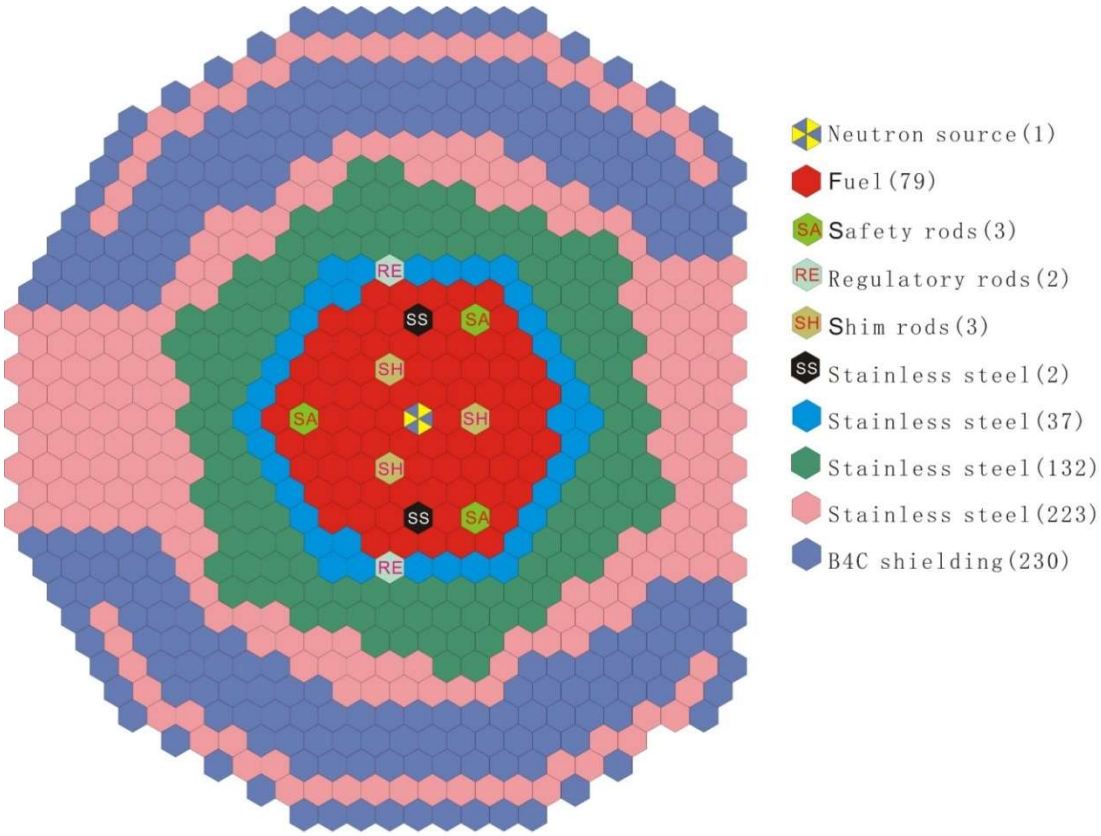

FIG. 2. The layout of the first loading

The core of first loading consists of 79 fuel subassemblies (abbr. SA), 8 control SAs, one neutron source SA, 394 stainless steel (abbr. SS) SAs, and 230 boron shielding SAs. The 2 SS SAs in the fuel region, which are used to compensate for the residual reactivity of the fresh fuel in the first loading, will be replaced by 2 fuel SAs in the equilibrium refuelling cycle. The external shape and dimension of all SAs are almost the same, while the inner structure varies upon the specific SA type. The main design values of each type of SAs are listed in TABLE 2.

It should be noted that all the geometric parameters of SAs are based on the installation state, in which all the materials are at a uniform temperature of 20°C. For other temperatures, such as the 250°C in which most of the physical start-up tests were conducted, the geometric parameters should be calculated by use of the linear expansion coefficients of each material, listed in TABLE 3.

Multiple types of stainless steel are used as structure material, including 15-15Ti, 316Ti, 302, 304, etc. The key components of the active core subassemblies, such as the cladding and spacer wires, are made of 15-15Ti.

TABLE 2. MAIN PARAMETERS OF CORE SAs *

	Fuel SA		Control SA		SS SA		Boron Shielding SA	Neutron Source SA
	Fuel	blanket	Regulating	Shim, safety	Type I&II	Type III&IV		
Number of SAs in core (operation loading)	79		2	3+3	39	355	230	1
Length of SA, mm	2592		2580		2592	2592	2592	2580
Mass of SA, kg	29~31		22~23		41~43	42~44	31~33	39~41
Number of rods	61		7		7	1	7	7(1)

Rod lattice pitch, mm	6.95		15.5		20.6	N/A	20.15	20.7
Outer diameter of rod/cladding, mm	6.00		14.9		20.0	54.0	19.2	20
Inner diameter of cladding, mm	5.40		12.9		N/A(2)	N/A(2)	17.2	N/A
Diameter of spacer wire, mm	0.95		1.3×0.6(3)		0.6	N/A	0.95	1.3×0.6(3)
Screw pitch of spacer wire, mm	100		100		100	N/A	100	100
Effective material and enrichment	UO_2		B_4C		SS	SS	B_4C, 19.8a%^{10}B(Natural)	Cf-252
	64.4±0.5, wt%	0.3~0.72, wt%	19.6a%^{10}B (Natural)	92.0a%^{10}B				
Total mass of UO2 or B4C in each SA (kg)	5.30±0.13	1.28/ 3.23(4)	0.87		N/A	N/A	2.43	0.43E-6
Length of effective material, mm	450	100/ 250(5)	510		N/A	N/A	800	N/A

* All the parameters are corresponding to first loading, at installation temperature of 20℃, and in nominal value or design value.
(1): There is one rod containing neutron source, with another 6 SS rods surrounding it;
(2): The SS rod has no cladding;
(3): The spacer wire is ellipse, and the major axis is 1.3mm and the minor axis 0.6mm;
(4): The total mass of UO_2 is 1.28kg in upper blanket and 3.23kg in lower blanket of each SA;
(5): The length of upper blanket is 100mm, and the lower 250mm.

TABLE 3. LINEAR EXPANSION COEFFICIENTS

Material	Linear expansion coefficient
Fuel pellet	1.1×10^{-5}/°C
Blanket pellet	1.0×10^{-5}/°C
B_4C absorber	4.2×10^{-6}/°C
Stainless Steel	1.8×10^{-5}/°C

3. CORE SUBASSEMBLIES

3.1. Fuel SA

The geometry of fuel SA is shown in FIG. 3. Fuel SAs are of four types due to the difference in the nozzle structure, which is determined by the power of each SA and specific need for cooling. In each fuel SA there are 61 fuel rods. Radially, the rods are separated by spacer wires.

Both fuel and blanket pellets are cylinders made of sintered UO_2 powder. Below the pellets is the gas plenum to hold the gaseous fission products. The fuel rod is filled with helium gas at a pressure of about 2.6MPa. The design value of pellet density is provided in TABLE 4, as well as some other additional information of fuel pellets. The smeared density can be calculated by use of the total mass given in TABLE 5.

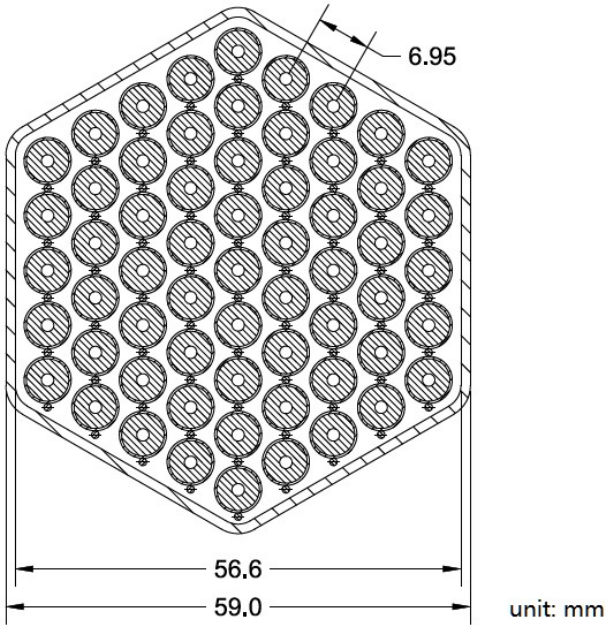

FIG. 3. The fuel SA

TABLE 4. ADDITIONAL INFORMATION OF FUEL ROD

	Fuel	Blanket
Diameter of pellet, mm	$5.20^{+0}_{-0.15}$	$5.20^{+0}_{-0.15}$
Diameter of central hole, mm	1.6±0.1	N/A
Design value of pellet density, g/cm3	10.5±0.2	≥10.3
Oxygen-to-metal (O/M) ratio	2.000~2.015	2.000~2.015
Pressure of helium gas, MPa	2.6	2.6

TABLE 5. TOTAL MASS OF FUEL/BLANKET IN EACH FUEL SA

		Design value	Measured Value			
			Average	Standard Deviation	Minimum	Maximum
Fuel	Mass of UO2, kg	5.30±0.13	5.28127	0.01295	5.2570	5.3421
	Mass of U, kg	4.66±0.12	4.64602	0.01167	4.6246	4.6979
	Mass of U-235, kg	N/A	2.98197	0.00852	2.9667	3.0156
	Enrichment of U-235, wt%	64.4±0.5	64.18315	0.09761	64.08	64.41
Blanket	Mass of UO2, kg	4.51±0.30	4.56629	0.01548	4.5345	4.6079
	Mass of U, kg	3.97±0.28	4.01855	0.01418	3.9940	4.0587
	Mass of U-235, kg	N/A	0.0179	3.1403E-4	0.0172	0.0183
	Enrichment of U-235, wt%	0.3~0.72	0.44532	0.00719	0.42924	0.45646

3.2. Control SA

The geometry of control SA is shown in FIG. 4. *The control rod*.

The reactivity of the reactor core is controlled by 8 control rod SAs: 2 regulating rod SAs (abbr. RE), 3 shim rod SAs (abbr. SH), and 3 safety rod SAs (abbr. SA).

In geometry and material, the three types of control SAs are almost the same; the differences only lie in two aspects: the enrichment of ^{10}B in B_4C absorber and the structure of nozzles. In neutronics calculation, the

difference of the nozzle will not make any difference, so all the control rod SAs share the same geometry model. In each control SA, there are 7 absorber rods.

The absorber rod consists of cladding, boron carbide (B_4C) pellets, plenum, upper and lower plugs. Different from a fuel rod, the absorber rod is open and allows the sodium to come inside and submerge the absorber pellets.

The B_4C in shim rods and safety rods contains enriched ^{10}B, while in regulating rods it is at natural abundance. The measured total mass of B_4C is given in TABLE 6.

As a basic provision, the term position of control rod (or simply rod position) is defined as the axial distance between the lower end of control rod absorber and the lower end of fuel. By this definition, the position of control rod at the operating full-insertion state is 0.

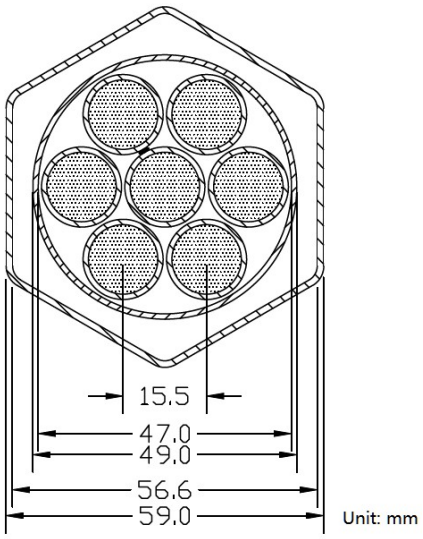

FIG. 4. The control rod

TABLE 6. TOTAL MASS OF ABSORBER IN EACH CONTROL SA

		Design Value	Measured Value			
			Average	Standard Deviation	Minimum	Maximum
Mass of B4C, kg		0.87±0.07	0.86545	0.00522	0.86	0.87
Mass of B-10, kg	Shim & Safety SAs	0.59±0.05	0.58625	0.00518	0.58	0.59
	Regulating SAs	0.119±0.04	0.11733	5.7735E-4	0.117	0.118

3.3. SS SA

The geometry of stainless steel (SS) SA is shown in FIG. 5.

SS SAs are used for the reflection of neutrons, and shielding for the outer structures. Due to the different positions in the core and different needs for cooling, SS SAs are divided into four types, between which the design of nozzle is different. In addition, the number of SS rods is different. Type-I or Type-II consists of 7 rods with a diameter of 20mm, while Type-III or Type-IV has only one rod with a diameter of 54mm.

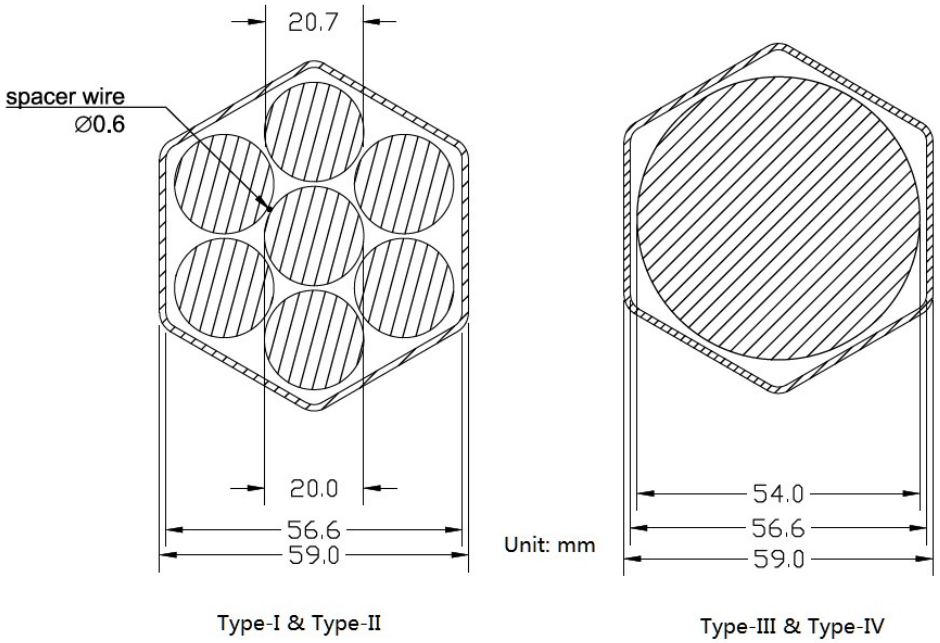

FIG. 5. The stainless steel SA

3.4. Boron Shielding SA

The geometry of boron shielding SA is shown in FIG. 6.

The shielding SA has a similar geometry with the Type-I and II SS SA. It consists of 7 absorber rods, which contain B_4C at natural abundance of ^{10}B. Similar to the control SA, the absorber rod in a boron shielding SA is also open and allows the sodium to come inside.

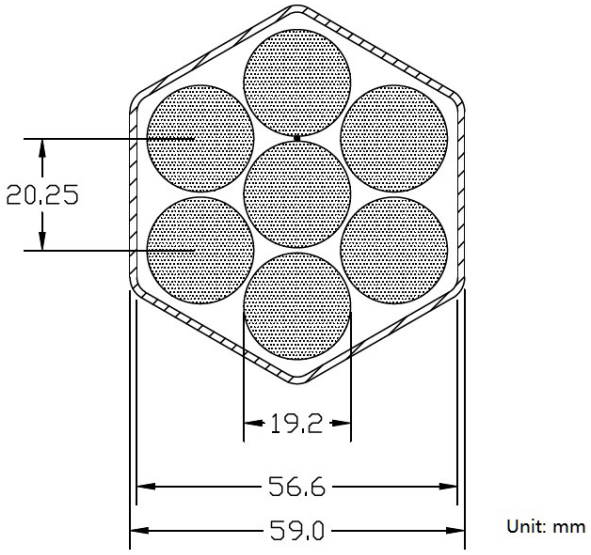

FIG. 6. The boron shielding SA

3.5. Other Subassemblies

In addition to the subassemblies described above, some other subassemblies are also needed for the commissioning, start-up, and all kinds of experiments.

The neutron source SA is used to improve the neutron flux in the subcritical state. It is loaded at the centre of the core and stays there under all operating conditions. The structure of the neutron source SA is almost the same with the Type-I and Type-II SS SA, with only a sealed ampoule containing 0.43mg of ^{252}Cf loaded in the central tube. The neutron source emits neutrons at a rate of 1.0×10^{9} n/s.

Before the fuel is loaded, the fuel positions are filled with mock-up subassemblies, which will be replaced by fuel SAs during physical start-up. The mock-up SAs are made of stainless steel rods, with the total mass and nozzles identical to those of the fuel SAs.

Several experimental SAs were used for irradiation of foils and for measurement of sodium void reactivity, etc. They were fabricated by making modifications on a fuel SA or an SS SA.

4. EXPERIMENT DESCRIPTION

During the physical start-up of CEFR, a series of experiments were carried out, some of which are selected for benchmark analysis introduced by this paper. All the experiments were expected to be conducted under cold state (also known as the refueling state), in which all core materials are at a uniform temperature of 250 ℃ nominally; however, the actual temperature may be several degrees away from the nominal value.

The start-up test was carried out in low power, and all the experiments involved in this benchmark are defined as low-power or zero-power experiments. Actually, for most of the measurement, the reactor power was controlled under 0.01% full-power; in the foil irradiation experiments, which need much higher flux, the power was believed to be below 0.1% full-power. The power limit was determined by measurement of starting point of nuclear heating; and it was found that the starting point of nuclear heating corresponds to a power of 59kW, i.e. 0.1% full-power.

4.1. Fuel loading and criticality

Before the start-up of the reactor, the core was preliminarily loaded with mock-up SAs in the fuel positions. The reactor reached first criticality by replacing mock-up SAs with real fuel SAs step by step; in each step, the number of fuel SAs to be loaded is determined by extrapolation of reciprocal of count rate and safety requirements. After the 72nd fuel SA was loaded, all other control rods were withdrawn to out-of-core position, while RE#2 (one of the two regulating SAs) was fully inserted; then RE#2 was withdrawn step by step to reach super-criticality, and in each position a positive period was obtained; the critical position of RE#2 was predicted by extrapolation based on the worth curve calculated. The final clean-core criticality state is that the core was loaded with 72 fuel SAs and the RE#2 rod was at the position of 70mm and the measured sodium temperature was 245 ℃. The measured reactivities of the final four steps while approaching criticality are shown in TABLE 7. The loading process is shown in FIG. 7.

The term clean core refers to the state that the criticality is reached by minimum fuel SAs and almost all the control rods are out of core, with only one regulating rod at a certain position to compensate for the small remaining positive reactivity due to the loading of the last fuel SA. After the above experiment, 7 more fuel SAs were loaded to reach the operation layout, in which all the 81 mock-up fuel SAs had been replaced by 79 fuel SAs and 2 Type-I SS SAs; the core reached criticality with the SH and RE rods at about core mid-plane. All other experiments introduced in this paper were conducted in the operation layout.

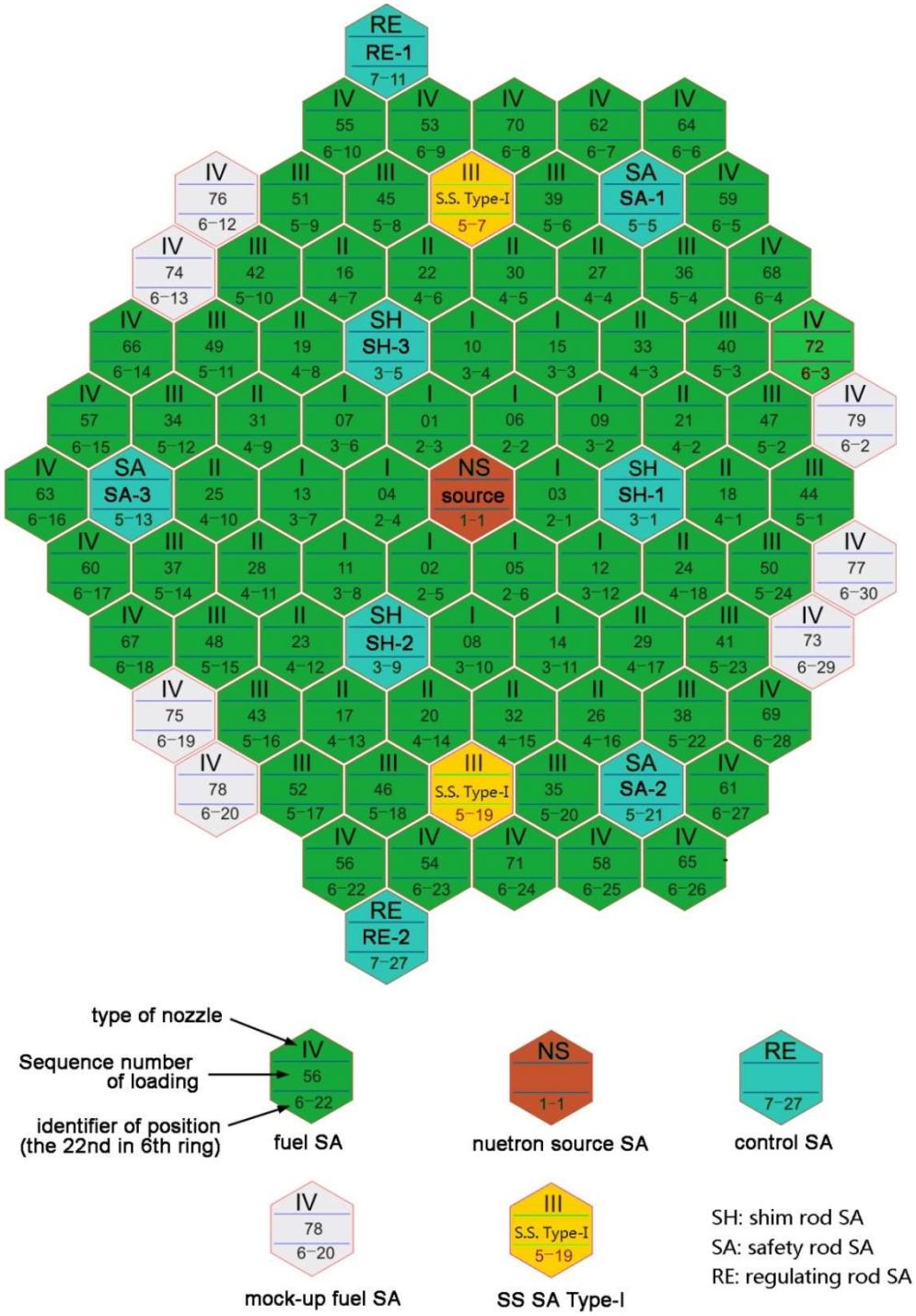

FIG. 7. The loading process of SAs

TABLE 7. Measured reactivities in approaching criticality

RE position (mm)	ρ(Δk/k) [pcm]
190	40
170	34
151	25
70	0 (estimated)

4.2. Control rod worth measurements

The measurement of control rod worth is an essential part of reactor start-up and provides important data for reactor operation and safety review. The experiment was carried out at operation layout. In control rod movement speed, both rod-drop and normal-speed movement were carried out; in calculation method, both inverse kinetics and period method were used; in control rod worth, both integral worth and differential worth were measured. The integral worth is defined as the total reactivity change when one or several control rods move from top to the bottom position. The differential worth is the reactivity change per unit length movement, which is usually in the form of an S curve.

In rod-drop measurement, by use of specially designed control logics one rod or any combination of rods can be dropped at the speed listed in TABLE 8. At the beginning of measurement, the rod to be measured was withdrawn to the out-of-core position; by moving other control rods, the core was kept at a certain positive reactivity, so that the neutron flux would increase; at the moment the count rate of detectors reached 30,000cps, the rod was dropped; the reactivity meter recorded the count rate and calculated the reactivity based on the inverse kinetics method by a time interval of 1.0s. The rod positions and measured worths of typical rods can be found in TABLE 9.

According to safety regulation, the three shim rod SAs and two regulating rod SAs make the first shut down system, while the three safety rod SAs make the second shut down system. To meet safety requirement, the worth of each shut down system was also measured. In addition, the shutdown margin should also be enough even one rod of largest worth was stuck; such cases were also measured.

TABLE 8. DETAILS OF MEASUREMENT OF CONTROL ROD WORTH

Movement speed	Calculation method	Control rod worth obtained	Control rod	Time of drop/s, or speed of normal movement/(mm/s)
Rod-drop	Inverse kinetics	Integral worth	RE	≤2.5
			SH	
			SA	≤0.7
Normal speed	Inverse kinetics & period method	Differential worth	RE	10
			SH	2±0.5
			SA	1±0.5

TABLE 9. EXPECTED OUTPUT OF CONTROL ROD WORTH MEASUREMENT

Measured rod(s)		Control rod positions/mm								Measured worth /pcm
		RE#1	RE#2	SH#1	SH#2	SH#3	SA#1	SA#2	SA#3	
RE#1	Before drop	**501**	106	240	240	239	498	500	500	150±9
	After drop	**-1**	106	240	240	239	498	500	500	
SH#1	Before drop	240	240	**501**	141	141	498	499	499	2019±250
	After drop	240	240	**4**	141	141	498	499	499	
SA#1	Before drop	240	239	240	240	241	**498**	499	499	945±100
	After drop	240	239	240	240	241	**46**	499	499	
SA#3	Before drop	240	239	240	240	240	498	499	**499**	946±98
	After drop	240	239	240	240	240	498	499	**40**	
All 8 rods	Before drop	**247**	**248**	**240**	**240**	**240**	**499**	**500**	**500**	6079±989
	After drop	**0**	**3**	**2**	**-2**	**0**	**45**	**56**	**40**	

4.3. Sodium void reactivity

The sodium void reactivity is obtained by replacing a fuel SA with a specially designed ‘voided’ SA and measuring the change of critical positions of control rods, whose differential worth was already known since the worth calibration had been done.

The experimental SA was the same as a fuel SA except that it was filled with gas and sealed by welding to simulate the sodium void. At the beginning of the experiment, the control rods were moved to reach criticality, and the rod positions were recorded as a basic state; then a fuel SA was replaced by the voided SA; the control rods were moved to regain criticality, and the new positions were recorded; the reactivity change caused by the voided SA was obtained by the change of positions of control rods and the worth curve already known. As the sodium void reactivity in one fuel SA is quite small, only RE rods were moved to compensate for the reactivity change, while the SH and SA rods were kept still throughout the measurements, whose positions are shown in TABLE 10.

Five fuel SAs were replaced one after another by the voided SA to obtain the sodium void reactivity in different positions of the core. The measured void reactivities are shown in TABLE 11, as well as the RE rods' positions.

TABLE 10. POSITIONS OF SHIM RODS AND SAFETY RODS

Control Rod		Position/mm
Shim rods	SH#1	239.3
	SH#2	239.2
	SH#3	239.8
Safety rods	SA#1	498.3
	SA#2	499.8
	SA#3	499.1

TABLE 11. EXPECTED OUTPUT OF VOID REACTIVITY MEASUREMENT

Measurement position in core		Control rod positions		Temperature/℃	Measured void reactivity/ pcm
		RE#1	RE#2		
(2-4)*	Original	277.6	277.3	248	-39.2±5.8
	Voided	336.8	336.8	247	
(3-7)	Original	278	277.4	248	-43.4±5.9
	Voided	337.9	337.9	248	
(4-9)	Original	277.7	277.6	248	-40.5±5.7
	Voided	338	337.6	248	
(5-11)	Original	278.4	276.2	248	-40.1±5.5
	Voided	338	337.5	248	
(6-13)	Original	302.9	303.3	248	-32.9±5.5
	Voided	338.1	337.8	248	

* The position could be found in FIG. 7.

4.4. Temperature reactivity

Fourteen thermal couples were installed above the reactor core to get the average outlet temperature of sodium, which was regarded as the uniform temperature of all materials. At each temperature step, it stayed for a long time so that a stable and uniform temperature distribution was reached.

The experiment method is similar to that of sodium void reactivity measurement. Firstly, at shutdown state the sodium temperature of reactor core was changed to a certain value and kept steady for at least half an hour; then the control rods were withdrawn to make the core close to critical state; the control rods were then inserted and the reactor was shut down; after that the temperature was changed to the next level and the previous steps were repeated, and a new set of control rod positions were measured. The actual measurement was conducted at 5 temperature levels by both increasing temperature from 250 to 300 °C and decreasing the temperature from 300 to 250 °C, so totally 10 sets of data were obtained, as is shown in TABLE 12.

TABLE 12. EXPECTED OUTPUT OF TEMPERATURE REACTIVITY MEASUREMENT

Measured Temperature/℃		Control rod positions*/mm					Measured reactivity coefficient/(pcm/℃)
		RE#1	RE#2	SH#1	SH#2	SH#3	
Increasing process	250	207.2	207.7	247.9	247.7	248.0	-3.76±0.56
	275	212.3	212.9	253.6	253.1	253.8	
	283	239.7	239.3	253.4	253.1	254.0	
	293	282.8	283.4	253.4	253.0	253.7	
	302	307.5	307.0	254.7	254.6	255.9	
Decreasing process	300	407.7	408.5	501.5	162.3	162.2	-4.38±0.66
	290	283.4	283.8	254.0	253.7	254.4	
	281	285.2	284.6	502.0	162.2	162.2	
	270	232.4	232.2	501.9	162.2	162.2	
	250	118.5	118.9	501.8	162.2	163.0	

* The SA rods were all out-of-core.

4.5. Subassembly swap reactivity

The SA swap measurement was aimed to simulate the possible fuel loading error, i.e. loading a fuel SA in an SS position or reversely. The measurement was carried out by change of critical positions of control rods as well. Eight SAs were selected for measurement, among which 6 were fuel SAs, and 2 were Type-I SS SAs. The position of the SAs and swap logics can be found in TABLE 13.

For the 6 fuel SAs, the measurement went as following. Firstly, the control rods were withdrawn and the critical positions were measured, after which the reactor was shut down again by inserting all control rods. Then the fuel SA in position (2-6), for example, was taken out of core, and a Type-I SS SA was loaded into that position. The control rods were withdrawn to find the new critical positions and the remaining small reactivity was measured by both inverse kinetics and period methods. The swap reactivity could be calculated based on the change of control rod positions and the measured reactivity.

However, the logics were different for the measurement of two SS SAs. To keep the reactor safe, a SS SA was not replaced by a fuel SA directly; instead, the measurement of a SS SA replacement is merged into a fuel SA replacement. For example, when position (5-23) was loaded with an SS SA and the reactivity measurement was completed, it was not recovered directly to hold the original fuel SA; instead, the fuel SA was swapped with the SS SA in position (5-19), and the reactivity change was measured. The same logic was used for position (6-29) and (7-31). The logics can be figured out by TABLE 13.

Therefore, generally it could be found that the whole experiment only took use of one SS SA that was out of core; no fuel SA outside was used. The number of fuel SAs loaded was never greater than 79 in the whole process, which is important to keep the reactor safe.

Each swap reactivity was measured both by one rod and by multiple rods. It is found that the difference between two cases is very small, therefore in this paper only the measured results by multiple rods are shown in TABLE 14.

TABLE 13. POSITIONS AND SA LOADING FOR SWAP REACTIVITY MEASUREMENT

Position to be measured*	SAs Loaded After Swap							
	(2-6)	(3-11)	(4-17)	(5-23)	(6-29)	(5-22)	(7-31)	(5-19)
(2-6)	SS	Fuel	Fuel	Fuel	Fuel	Fuel	SS	SS
(3-11)	Fuel	SS	Fuel	Fuel	Fuel	Fuel	SS	SS
(4-17)	Fuel	Fuel	SS	Fuel	Fuel	Fuel	SS	SS
(5-23)	Fuel	Fuel	Fuel	SS	Fuel	Fuel	SS	SS
(6-29)	Fuel	Fuel	Fuel	Fuel	SS	Fuel	SS	SS
(5-22)	Fuel	Fuel	Fuel	Fuel	Fuel	SS	SS	SS
(7-31)	Fuel	Fuel	Fuel	Fuel	SS	Fuel	Fuel	SS
(5-19)	Fuel	Fuel	Fuel	SS	Fuel	Fuel	SS	Fuel

* The position can be found in FIG. 7.

TABLE 14. EXPECTED OUTPUT FOR SWAP REACTIVITY MEASUREMENT BY MULTIPLE RODS

Measurement position		T/℃	Rod positions/mm					Measured reactivity/pcm
			RE#1	RE#2	SH#1	SH#2	SH#3	
(2-6)	Original	246	267.2	267.3	241.2	242.0	241.4	-986±128
	Swapped	246	326.7	325.2	297.6	297.2	299.0	
(3-11)	Original	246	257.6	257.1	241.5	241.7	242.0	-880±114
	Swapped	246	258.2	260.4	293.3	293.4	294.5	
(4-17)	Original	246	258.9	257.2	241.6	241.5	241.3	-777±101
	Swapped	246	257.1	257.7	288.2	288.9	288.7	
(5-23)	Original	246	257.7	257.1	241.1	241.1	241.3	-634±82
	Swapped	246	293.4	292.9	275.7	275.0	275.0	
(6-29)	Original	246	258.8	258.9	241.0	242.2	241.8	-474±62
	Swapped	246	317.9	317.0	277.7	277.2	278.5	
(5-22)	Original	246	319.1	317.2	277.7	277.2	278.6	-590±77
	Swapped	246	230.0	229.4	247.1	246.6	247.0	
(7-31)	Original	246	258.1	259.7	241.4	241.2	242.0	210±27
	Swapped	246	295.2	294.5	267.6	267.4	268.7	
(5-19)	Original	246	295.2	294.5	267.6	267.4	268.7	582±76
	Swapped	246	295.2	294.6	255.3	255.2	255.8	

4.6. Foil activation measurements

In CEFR an activation analysis laboratory was built, and by use of activation foils and specially designed irradiation SAs and devices, a series of measurements were conducted to obtain the reaction rate distribution, neutron spectrum, cross-section ratios, etc. Totally 202 foils were used for all kinds of measurements. Among all these experiments, the reaction rate measurement were included in this benchmark analysis, including foils of ^{235}U(n,f), ^{238}U(n,f), ^{237}Np(n,f), ^{197}Au(n, γ), ^{58}Ni(n,p), ^{27}Al(n, α).

The activation foils were enclosed in specially designed experimental SAs. They were loaded in 8 SA positions for measurement of radial reaction rate distribution, among which 5 positions are for fuel SAs and 3 for SS SAs, as is shown in FIG. 8. For the radial distribution calculation, the foil is supposed to be in the core mid-plane. Position #1 is also used for the measurement of axial distribution, in which the irradiation foils were fixed at 13 or 14 axial positions.

After irradiation in core, the activities of induced nuclides were measured by high-purity-germanium spectrometer; by mathematical treatment and normalization the relative reaction rates were obtained.

As only one experimental fuel SA was manufactured, the 5 radial positions were measured one after another. Each measurement consisted of SA swap, reactor start-up, shut down, cooling, uninstallation, etc, which took plenty of time. As the total time was limited, each operation or measurement was only conducted once, which brought in large possibility of experimental uncertainty. In such case, the powers of five measurements should be normalized, which was realized by the power monitoring foils located in a reserved position shown in FIG. 8. The experimental SA containing monitoring foils was loaded, taken out, and measured along with the experimental fuel SA in each measurement.

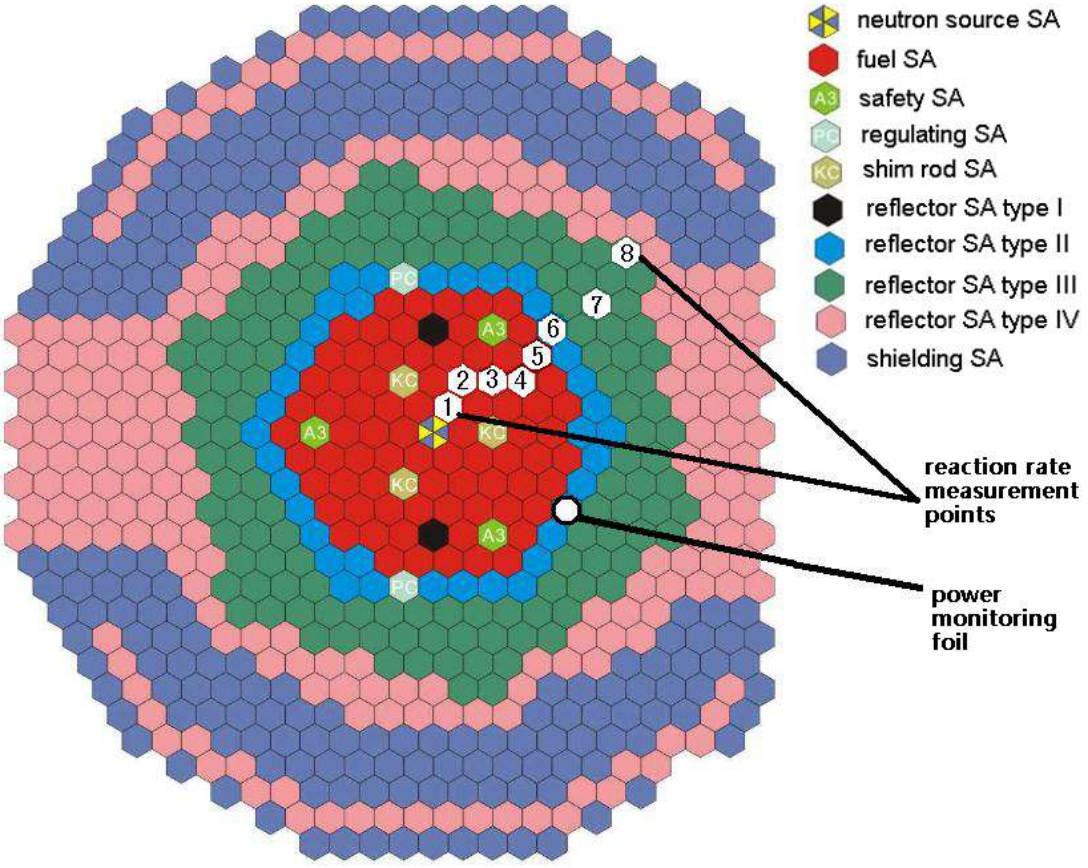

FIG. 8. Positions for reaction rate measurement

Each foil is a round thin plate made by stamping; a code was printed on each foil by laser. The mass of each foil was measured multiple times by a balance of 1/100,000 precision. The foils were grouped by mass and length of half-life, and then enclosed in aluminium wrapper and drawer, which was then vacuumed.

In order to reach the irradiation power as soon as possible, the reactor power was increased by a positive period of 60s, after which the reactor was kept in critical state for about 2 hours; after the irradiation, the reactor was shut down quickly by rod-drop. The irradiation power was below 0.1% nominal power.

6 reactions, including $^{235}U(n,f)$, $^{238}U(n,f)$, $^{237}Np(n,f)$, $^{197}Au(n,\gamma)$, $^{58}Ni(n,p)$, $^{27}Al(n,\alpha)$, were measured both radially and axially. To get the relative distribution, all the reaction rates are normalized to the central position, either axially or radially. The three safety rods (SA) were at out-of-core positions (500mm) in all reaction rate measurements.

TABLE 15 shows the control rod positions for measurement of radial distribution of reaction rates, and TABLE 16 shows the measured relative radial distribution of reaction rates; TABLE 17 shows the control rod positions for measurement of axial distribution of reaction rates, and TABLE 18 shows the measured relative axial distribution of reaction rates.

TABLE 15. CONTROL ROD POSITIONS FOR MEASUREMENT OF RADIAL DISTRIBUTION OF REACTION RATES

Measurement Position**	Control rod positions/mm				
	RE#1	RE#2	SH#1	SH#2	SH#3
#1 (2-2)	241	241	247	247	247
#2 (3-3)	222	222			
#3 (4-3)	198	199			
#4 (5-3)	172	172			
#5 (6-4)	147	149			

#6 (7-5)	147	149			
#7 (9-6)	147	149			
#8 (11-8)	147	149			

* This table corresponds to all six reactions described above;
** The serial number of position is indicated in Figure 15, and the number in brackets can be found in Figure 14;

TABLE 16. THE MEASURED RELATIVE RADIAL DISTRIBUTION OF REACTION RATES

Measurement position	235U(n,f)	238U(n,f)	237Np(n,f)	197Au(n, g)	58Ni(n,p)	27Al(n, a)
#1 (2-2)	1.00E+00	1.00E+00	1.00E+00	1.00E+00	1.00E+00	1.00E+00
#2 (3-3)	8.96E-01	9.64E-01	9.61E-01	9.39E-01	9.58E-01	9.66E-01
#3 (4-3)	8.44E-01	9.16E-01	9.08E-01	9.26E-01	9.39E-01	9.05E-01
#4 (5-3)	8.02E-01	8.42E-01	8.01E-01	8.64E-01	7.93E-01	8.23E-01
#5 (6-4)	6.48E-01	6.07E-01	5.80E-01	9.96E-01	5.86E-01	5.80E-01
#6 (7-5)	7.33E-01	2.61E-01	3.38E-01	2.37E+00	2.25E-01	2.00E-01
#7 (9-6)	7.17E-01	5.49E-02	9.21E-02	4.01E+00	3.47E-02	2.81E-02
#8 (11-8)	3.99E-01	1.38E-02	1.82E-02	2.34E+00	5.22E-03	4.14E-03

TABLE 17. CONTROL ROD POSITIONS FOR MEASUREMENT OF AXIAL DISTRIBUTION OF REACTION RATES (UNIT: MM)

RE#1	RE#2	SH#1	SH#2	SH#3
247	246	247	247	247

TABLE 18. THE MEASURED RELATIVE AXIAL DISTRIBUTION OF REACTION RATES

Axial Position/mm (relative to core center)	Measured Relative Reaction Rate					
	235U(n,f)	238U(n,f)	237Np (n,f)	197Au (n, g)	58Ni(n,p)	27Al(n, a)
300	4.24E-01	1.16E-01	1.08E-01	1.32E+00	8.03E-02	8.86E-02
250	4.89E-01	1.16E-01	2.09E-01	1.08E+00	1.57E-01	1.79E-01
200	5.99E-01	4.36E-01	3.80E-01	8.80E-01	3.32E-01	4.12E-01
100	7.93E-01	7.91E-01	7.28E-01	8.13E-01	7.75E-01	8.11E-01
50	9.16E-01	9.17E-01	8.74E-01	8.97E-01	8.95E-01	8.99E-01
0	9.67E-01	9.50E-01	9.55E-01	9.61E-01	9.79E-01	9.63E-01
-25	9.79E-01	9.79E-01	9.84E-01	9.88E-01	9.97E-01	1.00E+00
-50	1.00E+00	1.00E+00	1.00E+00	1.00E+00	1.01E+00	9.87E-01
-100	9.94E-01	9.35E-01	9.62E-01	1.01E+00	9.75E-01	9.46E-01
-150	9.40E-01		8.82E-01	1.01E+00	8.86E-01	
-200	8.55E-01	6.98E-01	7.39E-01	1.08E+00	6.96E-01	6.87E-01
-250	7.87E-01	3.68E-01	4.31E-01	1.35E+00	3.60E-01	3.25E-01
-350	6.52E-01	1.14E-01	1.30E-01	1.67E+00	9.70E-02	8.66E-02
-425	5.24E-01	5.08E-02		1.72E+00	4.04E-02	3.66E-02

5. SUMMARY AND CONCLUSION

In the physical start-up of CEFR, a series of neutronics experiments were conducted to obtain important physical characteristics of the core. This paper introduces the procedures and typical measurement results of criticality, control rod worth, temperature reactivity coefficient, subassembly swap reactivity, and reaction rate distribution. The core specifications and measurement results can benefit the neutronics field for validation of neutronics code and nuclear data.

ABBREVIATIONS

CEFR	China Experimental Fast Reactor
SA	subassembly
SS	stainless steel
RE	regulating control rod subassembly
SH	shim control rod subassembly
SA	safety control rod subassembly

ACKNOWLEDGEMENTS

The data and information presented in the paper are part of an ongoing IAEA coordinated research project on “Neutronics Benchmark of CEFR Start-Up Tests – CRP-I31032.

REFERENCES

[1] Huo, X., Hu, Y., Chen, Xiaoliang, Xu, L., Zhang, J., Chen, Xiaoxian, Cao, P., 2019. Technical Specifications for neutronics benchmark of CEFR start-up tests (IAEA CRP-I31032). China Institute of Atomic Energy.
[2] The neutronics benchmark of CEFR start-up tests, IAEA TECDOC (IAEA CRP-I31032) (under development)